

Mach reflection in detonations propagating through a gas with a concentration gradient

F. Ettner · K. G. Vollmer · T. Sattelmayer

Received: 19 October 2011 / Revised: 7 May 2012 / Accepted: 9 May 2012 / Published online: 14 June 2012
© Springer-Verlag 2012

Abstract In accident scenarios where detonations can occur a concentration gradient constitutes a more realistic initial condition than a perfectly homogeneous mixture. In this paper, the influence of a concentration gradient on detonation front shape, detonation instabilities and pressure distribution is studied. First, a simple method to determine the front shape from a given fuel distribution is presented. It is based on Huygens' principle and includes a correction to satisfy the boundary conditions on the enclosing walls. Next, the presented highly resolved Euler computations demonstrate the influence of a concentration gradient on detonation instabilities. In configurations with a strong concentration gradient, Mach reflection occurs and leads to an asymmetric pressure load on the enclosing geometry. In this case, the impulse on the wall is higher than in configurations with homogeneous fuel distribution, although the fuel content is much lower.

Keywords Detonation · Concentration gradient · Mach reflection · Nuclear safety · Hydrogen

1 Introduction

When hydrogen is released in accident scenarios it is very likely to form a vertical concentration gradient with the ox-

idant, mainly due to its low molecular weight. Especially in large geometries, such as reactor buildings, concentration gradients can remain stable for a surprising length of time, even when convection is present [1]. Although safety studies see an urgent need to investigate detonation propagation in inhomogeneous mixtures of this kind [2], hardly any fundamental research has been done in this field, so far.

For experimental and numerical analysis of detonations, it is important to differ between a concentration gradient parallel to the direction of reaction propagation and a concentration gradient perpendicular (transversal) to it. Thomas et al. [3] studied the probability of failure and reignition of a detonation when being transmitted through a concentration gradient parallel to it or through a layer of inert gas. A profound theoretical treatment of detonation propagation through parallel gradients has been given by Vidal [4]. The influence of transversal concentration gradients on flame acceleration and deflagration-to-detonation transition in tubes has previously been investigated by the authors [5–7]. Concerning the propagation of a fully developed detonation, Kessler et al. [8,9] studied the behavior of transverse instabilities and the probability of quenching using a one-step reaction model. Ishii and Kojima [10] have shown experimentally how a concentration gradient affects the shape of the detonation front and the detonation instabilities. Both the front shape and the instabilities under the influence of transversal gradients are investigated in this paper in more detail.

To compute the detonation front shape neglecting instabilities, the level set method [11,12] is a valuable tool. This method tracks the motion of an $n-1$ -dimensional surface in an n -dimensional domain at very low computational costs. The method is based on Huygens' principle assuming that a detonation front represents an infinitely thin discontinuity (wave) and each point on the wave front acts as a source for a new wave. The level set method is usually extended to

Communicated by L. Bauwens.

This paper is based on work that was presented at the 23rd International Colloquium on the Dynamics of Explosions and Reactive Systems, Irvine, California, USA, 24–29 July 2011.

F. Ettner (✉) · K. G. Vollmer · T. Sattelmayer
Lehrstuhl für Thermodynamik, Technische Universität München,
85747 Garching, Germany
e-mail: ettner@td.mw.tum.de

account for the effect of curvature on the propagation speed of the wave, and can further be improved by including even the derivative of the curvature [13].

The simplest way to visualize detonation instabilities experimentally is the soot print technique [14, 15, 10] which produces a cellular pattern that is characteristic for the mixture under investigation. In numerical investigations, an analogon to soot prints can be generated by recording the maximum pressure history in a computational domain. This technique is applied here to visualize the influence of a concentration gradient on the detonation instabilities and the propagation of the detonation front.

Provided that the width of the detonation cells is much smaller than the height of the channel, $\lambda \ll h$, the investigation of the integral detonation front and the instabilities can be carried out in two separate steps. This procedure is applied in the present paper. In Sect. 2, a simple graphical tool to predict the shape of the reaction front is presented. In Sect. 3, the instabilities are investigated using numerical solution of the Euler equations. The conclusions are presented in Sect. 4.

2 Front shape reconstruction

We study a detonation propagating in a long, two-dimensional channel. The fuel concentration varies in the direction perpendicular to the channel axis. In particular, we consider a hydrogen–oxygen mixture which is stoichiometric at the top of the channel (hydrogen mole fraction $x_{\text{H}_2} = 66.7\%$) and has a linearly decreasing hydrogen content towards the bottom. First, we neglect the role of detonation instabilities and consider steadily propagating reaction fronts only. Assuming that the detonation propagates at any point with the local Chapman–Jouguet (CJ) velocity into the axial direction would lead to a continually increasing time lag between the arrival of the detonation front at the top and at the bottom of the channel. However, it can be shown that after an initial acceleration the curvature of the detonation front remains unchanged: assuming that any point in the reaction front is a source from which the detonation propagates into all directions at the local CJ velocity (Huygens' principle), the curvature of the leading detonation front can be determined iteratively: constructing the detonation front as the envelope

of all circular waves emanating from the detonation front formed in the previous iteration (with the radius of each circle being proportional to the local CJ velocity), a converged solution is quickly achieved. An example is displayed in Fig. 1, showing a case where the hydrogen content decreases linearly by 10 percentage points from the top to the bottom of the channel (corresponding to an almost linear decrease in CJ velocity). In this reconstruction method, the resulting propagation velocity of the entire detonation front is governed by the maximum CJ velocity within the inhomogeneous mixture. The method is the graphical equivalent of the level set equation [13]

$$\frac{\partial \psi}{\partial t} + D_n |\nabla \psi| = 0 \quad (1)$$

where $\psi = 0$ defines the location of the detonation front and the propagation speed D_n normal to the front is identified with the local CJ velocity D_{CJ} . Here, D_n depends on the local hydrogen content while the influence of curvature on propagation speed is neglected.

This is a very simple method for getting a first impression of the detonation front. However, it violates the boundary condition that the flow on the lower wall must always be parallel to the wall. The adjustment that will occur in the real flow can be explained using a second, very simple model: by splitting the detonation front into an inert leading shock and an infinitely thin heat release zone, three different ways of adjustment to the wall can be distinguished (see Fig. 2):

- Case A: if the deviation from a normal shock is small, the flow immediately behind the shock remains subsonic ($M_2 < 1$). In this case, the leading shock is bended in the vicinity of the wall to allow wall-parallel flow.
- Case B: if $M_2 > 1$ and the deflection angle θ_1 caused by the incident shock is small, it can be compensated by a reflected shock (deflection angle $\theta_2 = -\theta_1$).
- Case C: if $M_2 > 1$ and the deflection angle θ_1 is too large to be compensated by the reflected shock, the flow adjusts to the wall by developing a Mach stem.

An overview of some calculations for the hydrogen–oxygen case with increasing concentration gradient is given in

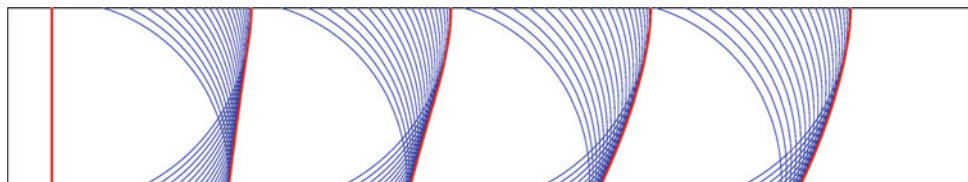


Fig. 1 Reconstruction of a detonation front in a medium with transversally varying CJ velocity using Huygens' principle. *Blue* circles emanating from the shock front with radius being proportional to the local

CJ velocity. *Red* detonation front defined as the envelope of all circles. Due to self-similarity of the problem, no length scale is given

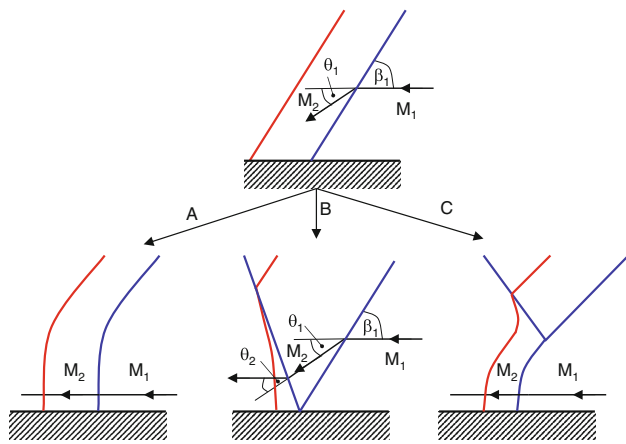


Fig. 2 Sketch of the problem (top) of non wall-parallel flow behind an oblique shock and the three possible solutions (bottom). Blue shocks. Red heat release zone

Table 1 Shock angles and Mach numbers gained with Huygens' method

Linear gradient	0 %	5 %	10 %	20 %
$x_{H_2,max}$	66.7 %	66.7 %	66.7 %	66.7 %
$x_{H_2,min}$	66.7 %	61.7 %	56.7 %	46.7 %
M_1	5.32	5.65	5.96	6.52
β_1	90°	72°	66°	47°
M_2	0.41	0.81	1.04	1.40
θ_1	0°	41°	42°	40°
$\theta_{2,max}$	–	–	–0.4°	–10°
Case	A	A	C	C

Table 1. It contains the Mach number M_1 and the incident angle β_1 of the shock close to the lower wall (where the hydrogen content is minimal), gained with the method shown in Fig. 1. From these quantities, the deflection angle θ_1 and the post-shock Mach number M_2 are computed using the oblique shock relations [16]. If $M_2 > 1$, the maximum deflection angle $\theta_{2,max}$ that can be achieved with a reflected shock is computed as well. It can be observed that in the case with a 10 % concentration gradient, the Mach number behind the leading shock just exceeds unity, so that $\theta_{2,max}$ is very small and the transition from case A to case C occurs. For higher concentration gradients as well, it can be seen that $|\theta_{2,max}| \ll |\theta_1|$ so that regular reflection (case B) never occurs in this configuration. Further calculations showed that regular reflection can only be expected in mixtures with low heat release (leading to low Mach numbers M_1) and extreme concentration gradients (leading to high incident angles $\beta_1 \ll 90^\circ$).

3 Simulation results

The real structure of a detonation front is more complicated than in the theoretical investigations shown so far, as instabil-

ities perturb the leading shock. To study the effect of instabilities, we numerically solve the reactive Euler equations for a mixture with N species in two dimensions:

$$\frac{\partial}{\partial t} \rho + \frac{\partial}{\partial x_i} (\rho u_i) = 0 \tag{2}$$

$$\frac{\partial}{\partial t} (\rho u_j) + \frac{\partial}{\partial x_i} (\rho u_i u_j) = -\frac{\partial p}{\partial x_j}, \quad j = 1, 2 \tag{3}$$

$$\frac{\partial}{\partial t} (\rho e_t) + \frac{\partial}{\partial x_i} \left(\rho u_i \left(e_t + \frac{p}{\rho} \right) \right) = 0 \tag{4}$$

$$\frac{\partial}{\partial t} (\rho y_n) + \frac{\partial}{\partial x_i} (\rho u_i y_n) = \dot{\omega}_n, \quad n = 1 \dots N - 1 \tag{5}$$

Here, ρ is the density, u the velocity and p the pressure of the gas. y_n represents the mass fraction of species n and $\dot{\omega}_n$ its reaction rate. The total energy e_t is defined as

$$e_t = \sum_{n=1}^N y_n \left(e_{f,n} + \int_{T_{ref}}^T c_{v,n}(T) dT \right) + \frac{u^2}{2} \tag{6}$$

$e_{f,n}$ is the energy of formation of species n at temperature T_{ref} and $c_{v,n}(T)$ is its temperature-dependent specific heat capacity at constant volume.

The equation of state is the perfect gas equation

$$p = \rho RT \tag{7}$$

and the mass fraction of the N th species can be computed as

$$y_N = 1 - \sum_{n=1}^{N-1} y_n \tag{8}$$

The fluxes are computed with a high resolution, Godunov-type central scheme [17].

Initially, the gas is at a temperature of 293 K and a pressure of 0.1 MPa. It is ignited by setting the state variables in a 2 mm wide region to the CJ values of a stoichiometric hydrogen–oxygen mixture. Different fuel concentration gradients within the unburned gas have been examined.

To study the detonation instabilities, two different models for the fluid were used. In the first model, all gas properties are assumed to be constant (notably the molecular weight W and the ratio of specific heats γ). There exist only two species ($N = 2$), the fuel and the products, that differ only in their enthalpy of formation. This corresponds to a specific heat release q being proportional to the local amount of fuel. The reaction rate $\dot{\omega}_{fuel}$ is modelled as a one-step irreversible Arrhenius reaction. In this model, it can be shown that the CJ velocity D_{CJ} varies according to

$$D_{CJ} \sim \sqrt{q} \sim \sqrt{y_{fuel}} \tag{9}$$

[18]. The problem in this model is that the Mach number of a CJ detonation also varies with $\sqrt{y_{fuel}}$, as the sound speed in the unburned mixture is constant, while in reality the sound speed depends heavily on gas composition. Consequently,

this model which has successfully been applied to many problems in homogeneous mixtures does not reproduce the real effects and therefore never showed Mach reflection in any of the cases studied.

In the second model, it was tried to reach a more realistic coupling between gas dynamics and heat release by defining the gas as a multi-component mixture consisting of the species H_2 , O_2 , H_2O , O , H , OH , HO_2 and H_2O_2 ($N = 8$). The temperature-dependent mixture properties are taken from the Chemkin thermodynamic database [19]. The chemical reaction is modelled using the mechanism by O'Conaire et al. [20].

Previous tests had shown that this model is able to reproduce the ignition length and the related one-dimensional parameters relatively well, but tends to considerably underestimate the cell size λ . The model was used to study the four cases from Table 1. It has been found that a uniform grid spacing of $\Delta x = \Delta y = 0.01$ mm was necessary to achieve grid independence. The domain height was chosen to be $h = 2$ mm.

The results are shown in Fig. 3. In the homogeneous case, the instabilities evolve as expected. Upwards and downwards running triple points intersect and leave a symmetric cellular pattern in the numerical soot print (maximum pressure history). In the case with a 5 % concentration gradient, the distortion of the detonation cells observed in the experiments by Ishii and Kojima [10] is reproduced. It can be explained by the locally varying velocity of the triple points caused by the locally varying hydrogen content. Instantaneous visualizations of the pressure show a detonation front which is inclined in the middle of the channel, but remains perpendicular in the vicinity of the channel walls. As expected from the theoretical investigations in Table 1, no reflections of the leading shock can be seen. In the case with a 10 % concentration gradient, reflection occurs via a Mach stem. It is relatively weak, as the theoretical Mach number behind the incident shock is just a little above unity, but causes a series of secondary reflections in the trailing flow behind the detonation. The distortion and the irregularity of the detonation cells in the numerical soot print in Fig. 3 increase compared to the 5 % case. In the case with a 20 % concentration gradient, the Mach stem can clearly be seen. It causes high pressure loads on the lower wall although the hydrogen content is much lower than in the upper part of the channel. The numerical soot print shows an interesting pattern: the downwards-running triple points produced by the detonation instabilities in the upper part of the channel are not reflected when they run into the Mach stem. Therefore, hardly any upwards-running triple points can be seen and the cellular pattern is replaced by unidirectional lines in some part of the channel. In the region behind the Mach stem, there are triple points running in both directions, but the cellular pattern is very small due to the increased compression compared to a planar CJ detonation.

The soot print can clearly be divided in a part caused by the instabilities behind the oblique shock and a part caused by the instabilities behind the Mach stem.

Concerning the propagation velocity of a detonation, an increasing velocity deficit with increasing concentration gradient is observed (up to 7 % velocity deficit for a 20 % concentration gradient compared to the homogeneous, stoichiometric case). However, it is important to note that the propagation velocity is still higher than the CJ velocity of a homogeneous mixture with the same hydrogen content.

For safety-related applications it is most important to determine the pressure loads on the enclosing walls. Therefore, pressure readings have been taken from the upper and the lower wall. The results for the 20 % gradient case are shown in Fig. 4. The blue lines show the pressure over time for several probes located next to each other on the upper wall. The maximum pressure can reach up to 60 bar, which is far above the von-Neumann pressure in a CJ detonation ($p_{vN} = 34$ bar in a stoichiometric mixture). Using more probes, a periodic fluctuation in the maximum pressure can be observed, where those probes hit by triple points observe the highest pressures. Shortly after the detonation front has passed, the pressure relaxes to approximately 15 bar which is close to the CJ pressure ($p_{CJ} = 19$ bar in a stoichiometric mixture). On the lower wall, nearly the same maximum pressures are experienced. However, as the pressure peaks are very short, a more valuable means of measuring the pressure load is the impulse

$$I = \int p A dt \quad (10)$$

which is obviously higher on the lower wall although there is less hydrogen driving the detonation. However, the explanation for this phenomenon is straightforward: as the detonation front velocity is mainly determined by the maximum hydrogen content at the upper wall, the detonation at the lower wall is not a CJ detonation, but an overdriven one. The Mach reflection causes a high pressure zone behind the leading shock which prevails for a longer time than in the upper part of the channel. This means that the destructive potential of a detonation running through a mixture with a transversal concentration gradient is higher than in a homogeneous mixture—even if compared to a homogeneous mixture that contains considerably more fuel.

4 Conclusions

The simplified analysis in Sect. 2 provides a simple tool for estimating detonation front curvature and reflection in a medium with a transversal concentration gradient. It is shown that for a hydrogen–oxygen mixture, the front adapts to the wall either by front bending or by Mach reflection. Regular

Fig. 3 Maximum pressure history (*left*) and instantaneous pressure field (*right*) in the multi-component simulation. The homogeneous case is shown on *top*, followed by increasing concentration gradient (5, 10, 20 %)

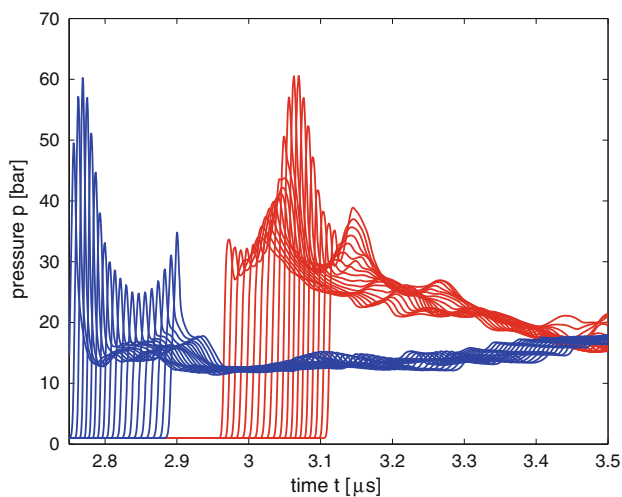
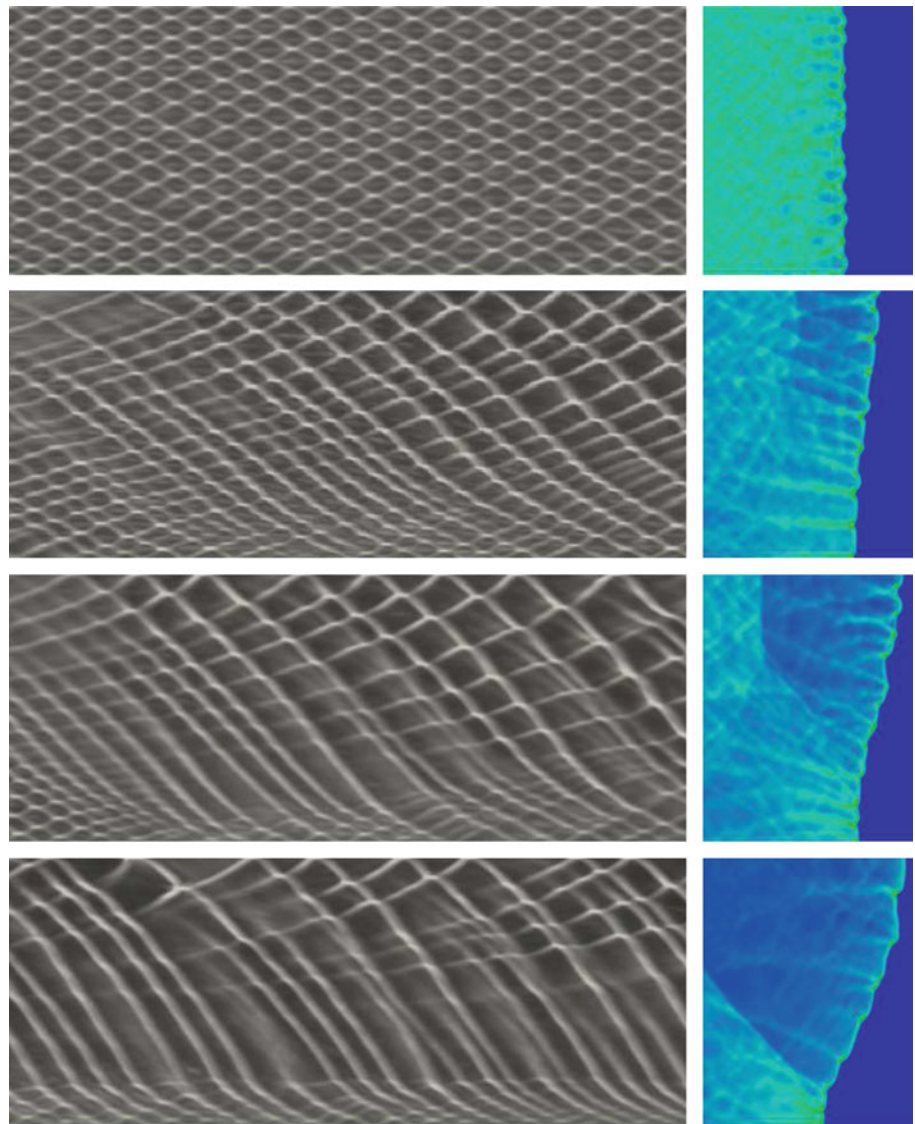


Fig. 4 Pressure recordings from the enclosing walls in the 20 % gradient case. *Blue* upper wall. *Red* lower wall

reflection is very unlikely to occur. These effects have been confirmed by Euler simulations. Additional effects have been revealed by the simulations, such as a very unusual soot print caused by Mach reflection in the case of a strong concentration gradient. In this case, the propagation velocities are between the CJ velocity of a homogeneous, stoichiometric mixture (corresponding to the maximum hydrogen content in the channel) and the CJ velocity of a homogeneous mixture with the same (average) hydrogen content as the inhomogeneous mixture. This velocity deficit is currently not accounted for in the model presented in Sect. 2, but could be incorporated by considering curvature effects (see [13]).

The pressure loads on the enclosing structure are asymmetric, with the higher impulse acting on the lower wall. It can be concluded that in the presence of a transversal concentration gradient, a fuel deficiency does not necessarily decrease the local pressure loads but can increase them.

The authors recommend to take this into consideration for future safety assessments.

Acknowledgments This project is funded by the German Federal Ministry of Economics and Technology on the basis of a decision by the German Bundestag (Project No. 1501338) which is gratefully acknowledged.

References

1. Auban, O., Zboray, R., Paladino, D.: Investigation of large-scale gas mixing and stratification phenomena related to LWR containment studies in the PANDA facility. *Nuclear Eng. Des.* **237**, 409–419 (2007)
2. Breitung, W., Chan, C.K., Dorofeev, S., Eder, A., Gerland, B., Heitsch, M., Klein, R., Malliakos, A., Shepherd, J.E., Studer, E., Thibault, P.: Flame acceleration and deflagration-to-detonation transition in nuclear safety. OECD State-of-the-Art Report NEA/CSNI/R(2000)7 (2000)
3. Thomas, G.O., Sutton, P., Edwards, D.H.: The behavior of detonation waves at concentration gradients. *Combust. Flame* **84**, 312–322 (1991)
4. Vidal, P.: Critical slow dynamics of detonation in a gas with non-uniform initial temperature and composition: a large-activation-energy analysis. *Int. J. Spray Combust. Dyn.* **1**, 435–471 (2009)
5. Ettner, F., Vollmer, K.G., Sattelmayer, T.: Numerical investigation of DDT in inhomogeneous hydrogen–air mixtures. In: Eighth International Symposium on Hazards, Prevention and Mitigation of Industrial Explosions, Yokohama, Japan (2010)
6. Vollmer, K.G., Ettner, F., Sattelmayer, T.: Influence of concentration gradients on flame acceleration in tubes. *Sci. Technol. Energ. Mater.* **72**, 74–77 (2011)
7. Vollmer, K.G., Ettner, F., Sattelmayer, T.: Deflagration-to-detonation transition in hydrogen–air mixtures with concentration gradients. In: 23rd International Colloquium on the Dynamics of Explosions and Reactive Systems, Irvine, CA, USA (2011)
8. Kessler, D.A., Gamezo, V.N., Oran, E.S.: Detonation propagation through a gradient in fuel composition. In: 23rd International Colloquium on the Dynamics of Explosions and Reactive Systems, Irvine, CA, USA (2011)
9. Kessler, D.A., Gamezo, V.N., Oran, E.S.: Gas-phase detonation propagation in mixture composition gradients. *Phil. Trans. Roy. Soc. A* **370**, 567–596 (2012)
10. Ishii, K., Kojima, M.: Behavior of detonation propagation in mixtures with concentration gradients. *Shock Waves* **17**, 95–102 (2007)
11. Osher, S., Sethian, J.A.: Fronts propagating with curvature-dependent speed: algorithms based on Hamilton–Jacobi formulations. *J. Comput. Phys.* **79**, 12–49 (1988)
12. Bdzil, J.B., Stewart, D.S.: Modeling two-dimensional detonations with detonation shock dynamics. In: Sixth Army Conference on Applied Mathematics and Computing, Boulder, CO, USA (1988)
13. Aslam, T.D., Stewart, D.S.: Detonation shock dynamics and comparisons with direct numerical simulations. *Combust. Theor. Model.* **3**, 77–101 (1999)
14. Denisov, Yu.N., Troshin, Ya.K.: On the mechanism of detonative combustion. *Symp. (Int.) Combust.* **8**, 600–610 (1961)
15. Guo, C., Wang, C., Xu, S., Zhang, H.: Cellular pattern evolution in gaseous detonation diffraction in a 90°-branched channel. *Combust. Flame* **148**, 89–99 (2007)
16. Anderson, J.D.: Modern compressible flow with historical perspective. pp. 133–138. McGraw-Hill, New York (2004)
17. Kurganov, A., Noelle, S., Petrova, G.: Semi discrete central-upwind schemes for hyperbolic conservation laws and Hamilton–Jacobi equations. *SIAM J. Sci. Comput.* **23**, 707–740 (2001)
18. Lee, J.H.S.: The detonation phenomenon. p. 44 Cambridge University Press, Cambridge (2008)
19. Kee, R.J., Rupley, F.M., Miller, J.A.: The Chemkin thermodynamic data base. Sandia Report SAND87-8215B (1991)
20. O’Conaire, M., Curran, H.J., Simmie, J.M., Pitz, W.J., Westbrook, C.K.: A comprehensive modeling study of hydrogen oxidation. *Int. J. Chem. Kinet.* **36**, 603–622 (2004)